

Article

Enhanced Corrosion Resistance of Carbon Steel in Hydrochloric Acid Solution by *Eriobotrya Japonica* Thunb. Leaf Extract: Electrochemical Study

Wenjing Yang ^{1,*}, Qihui Wang ¹, Ke Xu ¹, Yanjun Yin ¹, Hebin Bao ¹, Xueming Li ^{1,*}, Lidan Niu ² and Shiqi Chen ²

¹ College of Chemistry and Chemical Engineering, Chongqing University, Chongqing 401331, China; qihuiwang@cqu.edu.cn (Q.W.); ke.xu@cqu.edu.cn (K.X.); yanjunyin@cqu.edu.cn (Y.Y.); reformasky@cqu.edu.cn (H.B.)

² Chongqing Institute for food and Drug Control, Chongqing 401121, China; ldniu2@163.com (L.N.); chen1473@126.com (S.C.)

* Correspondence: yangwj308@cqu.edu.cn (W.Y.); xuemingli@cqu.edu.cn (X.L.)

Received: 19 July 2017; Accepted: 11 August 2017; Published: 16 August 2017

Abstract: The biodegradable inhibitors, which could effectively reduce the rate of corrosion of carbon steel, were investigated by potentiodynamic polarization and electrochemical impedance spectroscopy (EIS). The mixed-type inhibitors extracted from *Eriobotrya japonica* Thunb. leaf exhibited excellent inhibition performance, and the inhibition efficiency for carbon steel reached 90.0% at 298 K in hydrochloric acid. Moreover, the adsorption mechanism of the inhibitors on a carbon steel surface is described by the Langmuir adsorption isotherm. Simultaneously, the corrosion morphology of the carbon steel and the inhibitor structure were analyzed by scanning electron microscope (SEM) and Fourier transform infrared spectroscopy (FT-IR), respectively.

Keywords: carbon steel; *Eriobotrya japonica* Thunb.; corrosion inhibitor

1. Introduction

At present, various corrosion inhibitors such as inorganic and synthetic inhibitors have been employed in descaling and metal pickling processes [1,2]. However, their low bio-degradability and high cost severely limit their applications. Thus, the development of environmentally friendly, low-cost inhibitors is desirable and urgent [3,4]. Plant extracts are biodegradable in a natural environment, which allows them to serve as environmentally friendly inhibitors in acid solution [5]. Hydrochloric acid is one of the most widely used inorganic acids for metal pickling and descaling in industrial processes [6,7]. However, the acid is highly corrosive to metals and their alloys, especially for carbon steel (C-steel). Corrosion inhibitors have been extensively used to slow down the corrosion rate of C-steel [8]. Therefore, the development of plant extract inhibitors for C-steel pickling provides a new direction for these industrial processes. In recent years, green plant extracts of *morus alba pendula* [9], *Justicia gendarussa* [10], *Zenthoxylum alatum* [11], *Salvia officinalis* [12], *Ginkgo* [13], *Musa paradisiaca* [14], *Tagetes erecta* [15], Gum arabic [16], *Artemisia pallens* [17], lupine [18], *Jasminum nudiflorum* Lindl. [19], *Dendrocalamus brandisii* [20], aqueous garlic peel [21], henna [22], *Nypa fruticans* Wurmb [23], *Damsissa* [24], *Mentha pulegium* [25], olive [26], and *Nigella sativa* L. [27] have been widely studied and examined as effective inhibitors. However, to our knowledge, the corrosion inhibition behavior of *Eriobotrya japonica* Thunb. leaf extract (EJTLE) on C-steel in hydrochloric solution has not yet been reported.

Eriobotrya japonica Thunb. belongs to the genus *Rosa*, which is prevalent in most provinces of southern China. The fruit of this plant, one of the important subtropical fruits, and its leaves have

been used medicinally to treat coughs, colds, chronic bronchitis, phlegm, high fever, and gastro-enteric disorders [28].

The chemical composition of EJTLE largely consists of ursolic acid, oleanolic acid, and flavonoids. The molecular structures of ursolic acid [29], oleanolic acid, and flavonoids [30] are shown in Figure 1. These chemical constituents have anti-corrosion effects due to their heterocyclic structures and have been extensively researched. In general, these organic compounds contain heteroatoms such N, S, and O and are classified as heterocyclic compounds, which are regarded as effective adsorption centers.

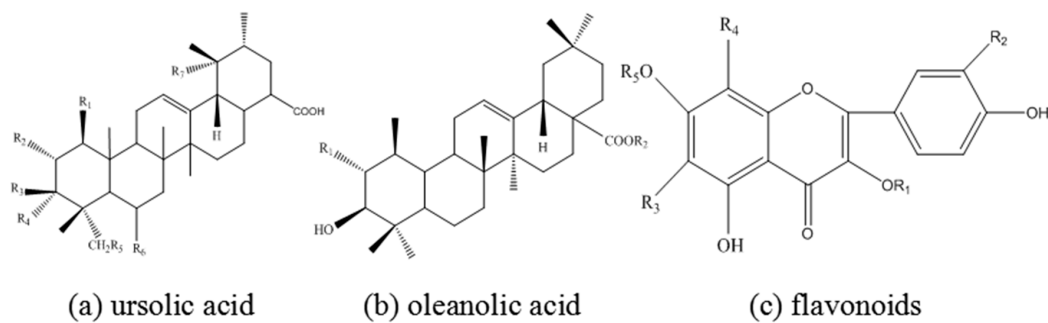


Figure 1. Molecular structures of (a) ursolic acid; (b) oleanolic acid; and (c) flavonoids.

In this work, the corrosion effect of EJTLE on C-steel was investigated by potentiodynamic polarization, electrochemical impedance spectroscopy (EIS), Fourier transform infrared spectroscopy (FT-IR), and scanning electronic microscopy (SEM). The adsorption behavior of EJTLE on the surface of carbon was also investigated.

2. Results

2.1. Open Circuit Potential Measurements

Figure 2 shows the open circuit potential curves of C-steel in 1 M HCl solution with different concentrations of EJTLE at different temperatures prior to electrochemical analysis. In Figure 2, the shape of the inhibition curves is similar to that of the uninhibited ones, suggesting that lower concentrations (below $0.06 \text{ g}\cdot\text{L}^{-1}$) of inhibitors did not significantly change the corrosion behavior of C-steel. Interestingly, the open circuit potential curve of carbon steel (C-steel) increases at first and then slowly decreases in the acid solution with higher concentrations of corrosion inhibitors (above $0.06 \text{ g}\cdot\text{L}^{-1}$). This phenomenon is related to the adsorption of inhibitors on the C-steel surface. The inhibitors contain heteroatoms and π bonds adsorbed on the electrode surface, resulting in higher electron density on the C-steel surface and negative electrode potential.

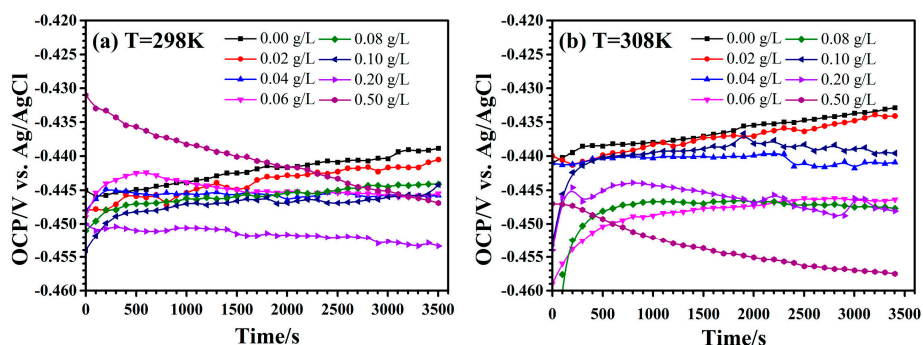


Figure 2. Cont.

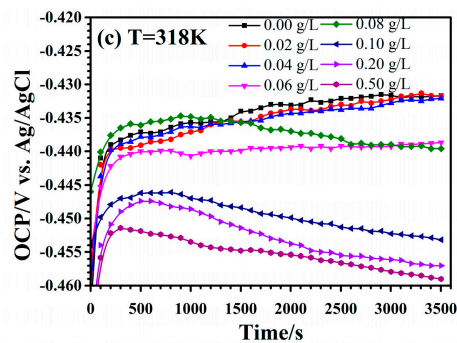


Figure 2. Open circuit potential curves of C-steel in 1 M HCl solution with different concentrations of *Eriobotrya japonica* Thunb. leaf extract (EJTLE) at (a) 298 K; (b) 308 K; and (c) 318 K.

2.2. Polarization Measurements

The polarization curves of C-steel in 1 M HCl solution at different temperatures are shown in Figure 3. As shown in Figure 3, the corrosion potential of C-steel in 1 M HCl acid is obviously negative, with an increasing concentration of corrosion inhibitors. In addition, the cathodic and anodic polarization curves exhibit low current density, meaning that the cathodic and anodic polarization reactions were inhibited. In order to show clearly the mechanism of corrosion inhibitors, cathodic polarization and anodic polarization are discussed separately. Compared with those of the blank solution, the cathodic polarization curves of C-steel with corrosion inhibitors did not change significantly. Similarly, the anodic polarization curves of C-steel with inhibitors were lower than the anodic polarization curves of C-steel in the blank solution. Additionally, the current plateaus in the anodic polarization curve, as expected.

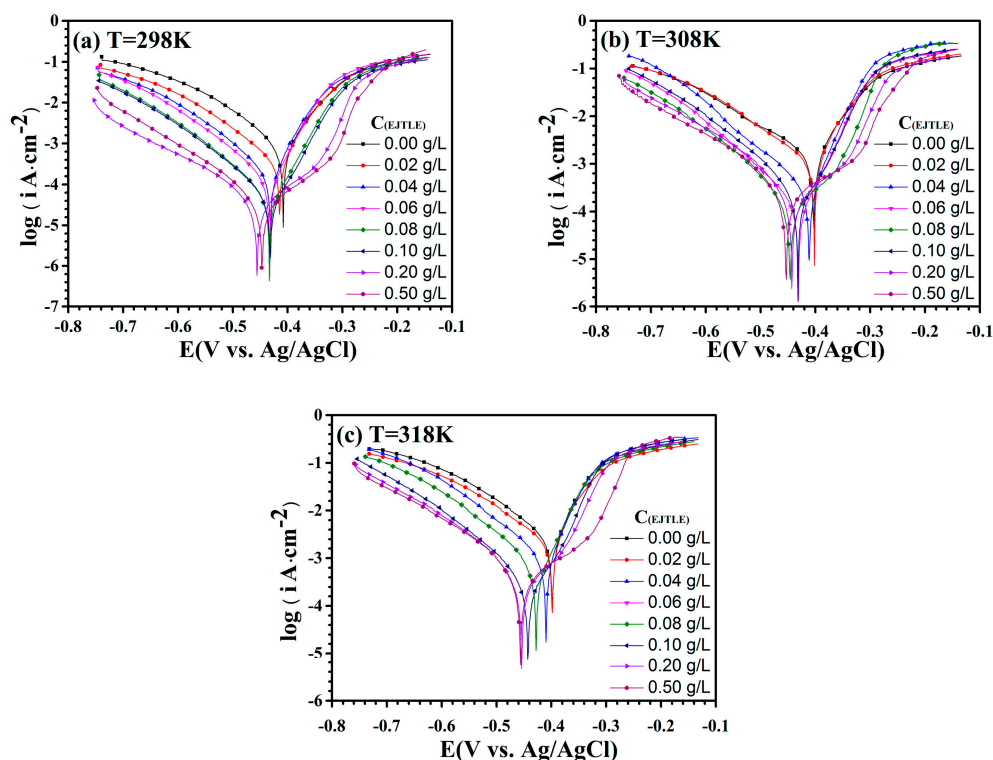


Figure 3. Polarization curves of C-steel in 1 M HCl solution with different concentrations of EJTLE at (a) 298 K; (b) 308 K; and (c) 318 K.

2.3. Electrochemical Impedance Spectroscopy

The Nyquist impedance plots and Bode plots of C-steel in 1 M HCl solution with and without different concentrations of EJTLE are shown in Figure 4. After the addition of inhibitors, the Nyquist and Bode diagrams of C-steel were similar to the Nyquist and Bode diagrams of the blank corrosion solution and only occurred as capacitive arcs. The capacitive arc reflects the relaxation process of the interface double layer and the charge transfer resistance. The diameter of the capacitive arc increases with increasing inhibitor concentration, which indicates that the corrosion of the C-steel electrode in 1 M HCl solution is inhibited. In combination with the corresponding Bode diagram, this means that the inhibited corrosion of C-steel was controlled by a time constant. Obviously, there is no Warburg impedance or inductive reactance arc in Nyquist plots.

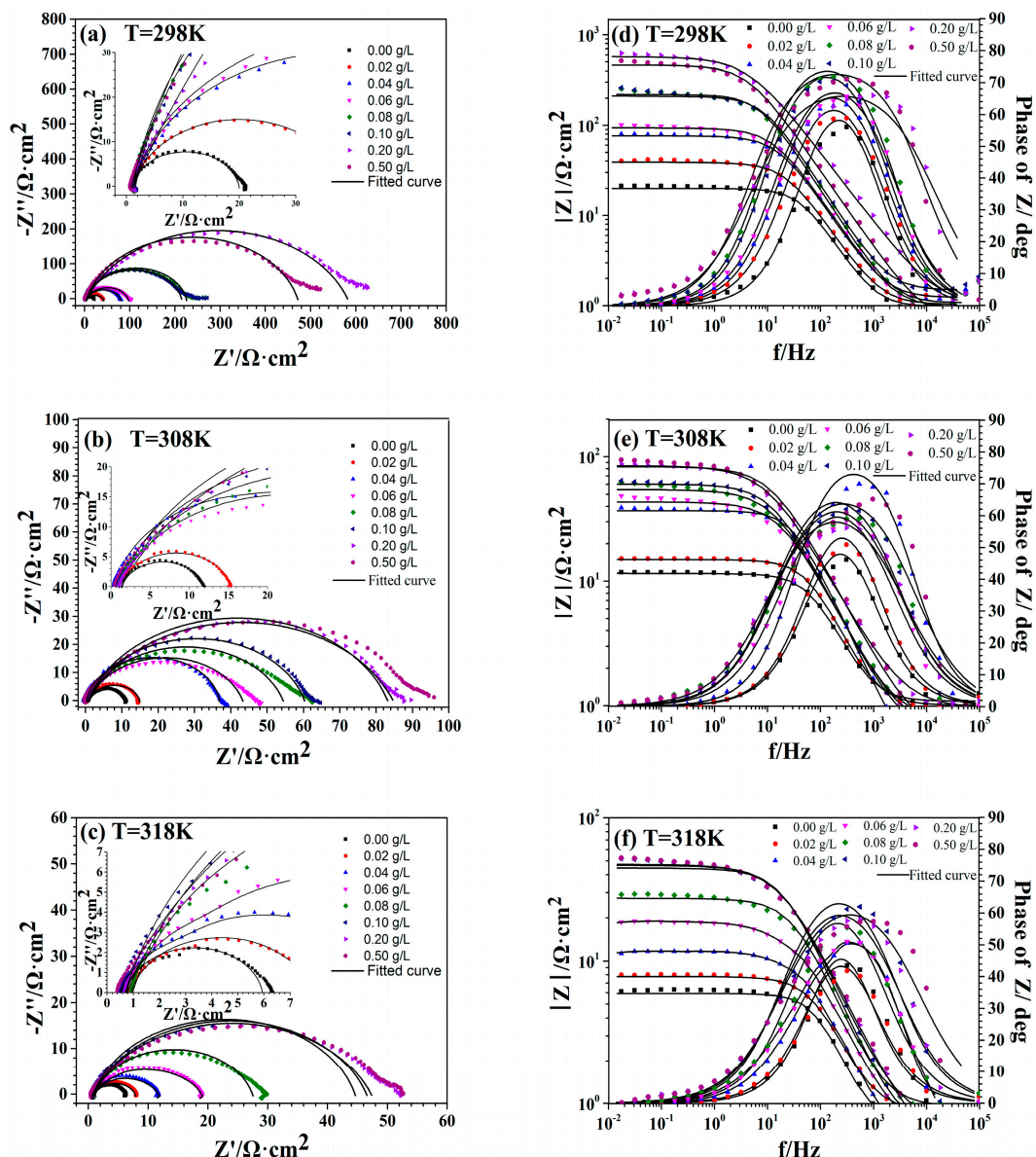


Figure 4. Nyquist plots (a) and Bode plots (b) of C-steel in 1 M HCl solution with different concentrations of EJTLE at 298 K; Nyquist plots (c) and Bode plots (d) of C-steel in 1 M HCl solution with different concentrations of EJTLE at 308 K; Nyquist plots (e) and Bode plots (f) of C-steel in 1 M HCl solution with different concentrations of EJTLE at 318 K.

We used the equivalent circuit model shown in Figure 5 to fit the data results of the electrochemical impedance spectroscopy (EIS). Figure 6 shows the variation of inhibition efficiency (η) in the presence of different concentrations of EJTLE at 298 K, 308 K, and 318 K. The inhibition efficiency of the plant inhibitors increased with increasing concentration. Additionally, the inhibition efficiency of the plant extract decreased as temperature increased. The results show that the plant inhibitors exhibit enhanced anti-corrosion performance, which can be used for high-efficient inhibitors in C-steel pickling and descaling processes.

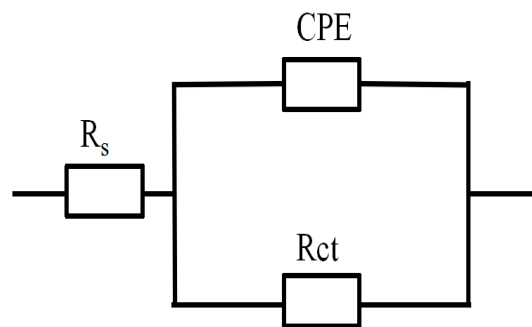


Figure 5. The equivalent circuit model used to fit the electrochemical impedance spectroscopy (EIS) data.

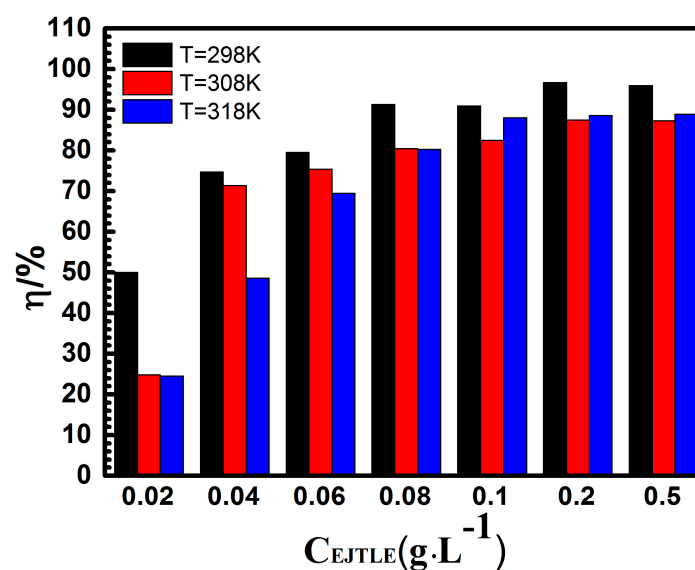


Figure 6. Variation of η in the presence of different concentrations of EJTLE at 298 K, 308 K, and 318 K.

2.4. Adsorption Isotherm

Generally, organic inhibitors have been accomplished by the adsorption of a protective film at the metal-solution interface, and the mechanism can be described by an adsorption isotherm. Figure 7 represents the fitting of C/θ versus C with a linearly dependent coefficient near 1.

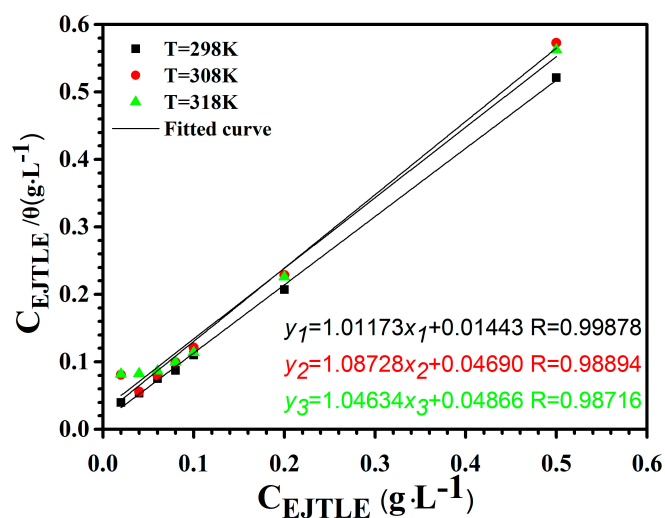


Figure 7. Langmuir adsorption isotherm of EJTLE on the C-steel surface in 1 M HCl solution at 298 K, 308 K and 318 K.

2.5. FT-IR Results

In order to characterize and confirm the product structure, FT-IR spectroscopy was performed. The FT-IR spectrum of EJTLE powder is shown in Figure 8. The strong band at 3421 cm^{-1} corresponds to the N–H or O–H stretching vibration. The band at 2927 cm^{-1} is related to the $-\text{CH}_2$ asymmetrical stretching vibration. The band at 1616 cm^{-1} is attributed to the C=C stretching vibration. The band at 1390 cm^{-1} could be assigned to the C–H bending in $-\text{CH}_3$. The adsorption band at 1073 cm^{-1} corresponds to the C–N or C–O stretching vibration. The band at 611 cm^{-1} can be assigned to C–H of aliphatic and aromatic carbon.

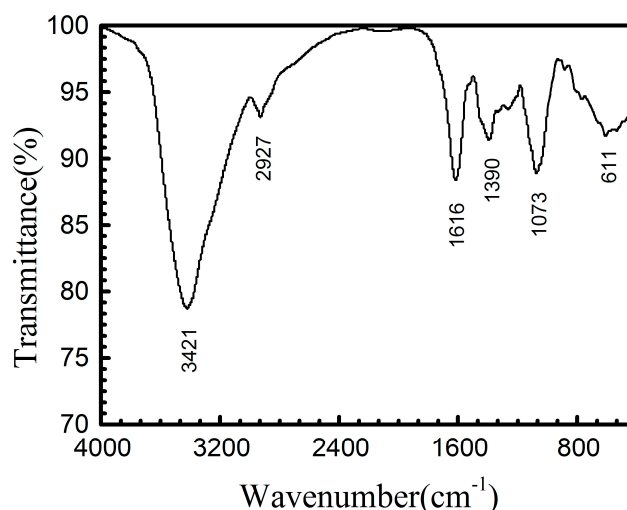


Figure 8. Fourier transform infrared spectroscopy (FT-IR) spectra of *Eriobotrya japonica* Thunb. leaf extract (EJTLE).

2.6. SEM Analysis

It can be seen from Figure 9 that the polished C-steel surface is smooth and without obvious scratches. Figure 10 shows the surface graphs of the C-steel surface exposed to 1 M HCl in the absence and presence of $0.5\text{ g}\cdot\text{L}^{-1}$ EJTLE at three temperatures. It can be clearly seen from Figure 10a–c that the rough surface with several grooves was caused by uniform corrosion in acid solution. Conversely, in

the presence of $0.5 \text{ g}\cdot\text{L}^{-1}$ plant inhibitors, the surface (Figure 10d–f) of C-steel shows relatively smooth polishing scratches. In light of these findings, we can conclude that the plant inhibitors do prevent the corrosion of carbon steel in 1 M HCl solution by the formation of adsorbed molecules on the surfaces of C-steel specimens.

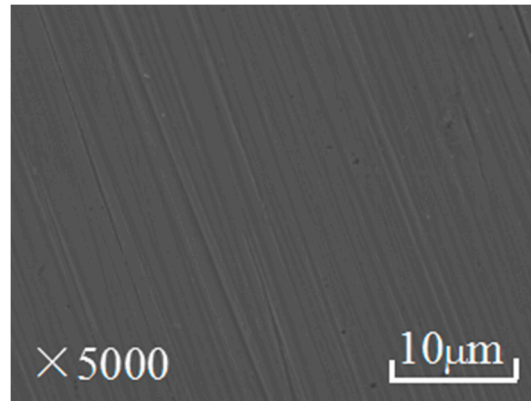


Figure 9. SEM images of the C-steel surface after sanding.

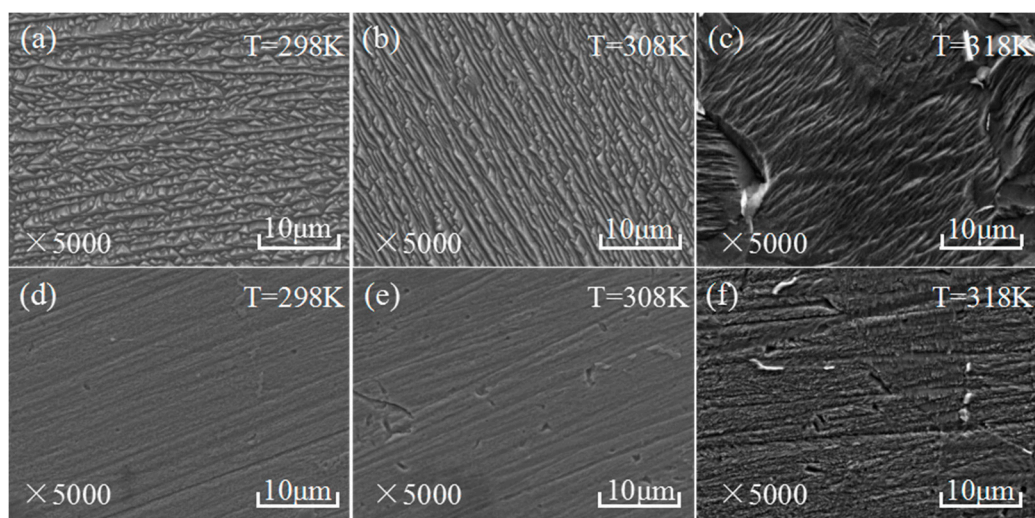


Figure 10. SEM images of the C-steel surface after immersion in 1 M HCl for 1 h: (a) at 298 K; (b) at 308 K; (c) at 318 K; (d) containing $0.5 \text{ g}\cdot\text{L}^{-1}$ EJTL at 298 K; (e) containing $0.5 \text{ g}\cdot\text{L}^{-1}$ EJTL at 308 K; and (f) containing $0.5 \text{ g}\cdot\text{L}^{-1}$ EJTL at 318 K.

3. Discussion

An extract was obtained from *Eriobotrya japonica* Thunb. leaves by immersing them in hot water at 363 K for 1 h. The properties of the extract as a corrosion inhibitor in an acid pickling solution were investigated by electrochemical experiments, SEM, and FT-IR.

In Figure 3, polarization curves show that the inhibitors can be considered mixed-type corrosion inhibitors because the corrosion potential was less than 85 mV [31,32]. Moreover, the plateau of the anodic polarization curves shows that the inhibitors desorbed from the C-steel surface. It is generally believed that this phenomenon indicates the formation of an adsorbed layer on the surface of C-steel, inhibiting cathodic hydrogen evolution and anodic iron dissolution. The inhibition efficiency can be calculated from the following equation:

$$\eta(\%) = \left(\frac{I_{\text{corr}}^0 - I_{\text{corr}}}{I_{\text{corr}}^0} \right) \times 100 \quad (1)$$

where I_{corr} and I_{corr}^0 are the corrosion current densities of C-steel with and without plant inhibitors, respectively.

The corrosion parameters calculated from Figure 3 are shown in Table 1. With increasing concentrations of plant extract, the corrosion potential of the electrode gradually shifted to a negative range of about 50 mV. When the inhibitor concentration was $0.1 \text{ g}\cdot\text{L}^{-1}$, the corrosion current density was $43.11 \mu\text{A}\cdot\text{cm}^{-2}$ at 298 K, and the corrosion inhibition efficiency reached 95.7%. When the temperature increased to 318 K, the corrosion inhibition efficiency was still above 85.0%. The inhibition efficiency of this plant inhibitor is relatively better than that reported in the literature. Obviously, the results show that the proper concentration of inhibitors (over $0.1 \text{ g}\cdot\text{L}^{-1}$) can significantly reduce the corrosion reaction during the pickling process of C-steel. Moreover, the protective mechanism of the extract is to form an adsorbed layer on the C-steel surface to inhibit the cathodic reduction reaction of H^+ and the anodic dissolution reaction of iron.

Table 1. Polarization parameters for C-steel in 1 M HCl solution with different concentrations of EJTLE at different temperatures.

Temperature (K)	CEJTLE ($\text{g}\cdot\text{L}^{-1}$)	E _{corr} (mV vs. Ag/AgCl)	B _c ($\text{mV}\cdot\text{dec}^{-1}$)	B _a ($\text{mV}\cdot\text{dec}^{-1}$)	I_{corr} ($\mu\text{A}\cdot\text{cm}^{-2}$)	η (%)
298	0	-408	-109	80	1006.00	-
	0.02	-415	-146	77	597.90	40.6
	0.04	-431	-96	67	229.50	77.2
	0.06	-433	-116	54	145.60	85.5
	0.08	-433	-92	50	47.92	95.2
	0.1	-432	-95	51	43.11	95.7
	0.2	-456	-76	91	28.88	97.1
	0.5	-447	-74	100	30.64	97.0
308	0	-403	-176	71	1864.00	-
	0.02	-402	-131	53	1194.00	35.9
	0.04	-411	-117	44	287.30	84.6
	0.06	-426	-106	53	229.20	87.7
	0.08	-433	-105	59	189.20	89.9
	0.1	-432	-107	59	206.20	88.9
	0.2	-443	-115	121	250.20	86.6
	0.5	-453	-92	157	245.90	86.8
318	0	-398	-121	52	2826.00	-
	0.02	-398	-120	47	2326.00	17.7
	0.04	-410	-117	48	1007.00	64.4
	0.06	-428	-120	45	546.00	80.7
	0.08	-429	-114	49	337.60	88.1
	0.1	-443	-108	58	265.50	90.6
	0.2	-454	-114	92	360.90	87.3
	0.5	-456	-123	125	461.60	83.7

Similarly, the EIS experiments also confirmed the results of the polarization experiments. The equivalent circuit model shown in Figure 5 was used to fit the EIS test parameters. As shown in Figure 5, R_s is the solution resistance, R_{ct} is the resistance of charge transfer, and the constant phase elements (CPE) are used to replace capacitance. The impedance values of CPE for the C-steel electrode in 1 M HCl solution is expressed as follows [8]:

$$Z_{\text{CPE}} = \frac{1}{Y_0(j\omega)^n} \quad (2)$$

In this expression, Y_0 is a proportional factor, ω represents the angular frequency ($\omega = 2\pi f$), n is the deviation parameter, and j is the imaginary unit. The capacitance of the electric double layer can be described as follows:

$$C_{dl} = \frac{Y_0\omega^{n-1}}{\sin(n\pi/2)} \quad (3)$$

The values of the inhibition efficiency can be calculated from R_{ct} by the following relationship:

$$\eta(\%) = \left(\frac{R_{ct} - R_{ct}^0}{R_{ct}} \right) \times 100 \quad (4)$$

where R_{ct} and R_{ct}^0 are the values of charge transfer resistance in 1 M HCl solution with and without EJTLE inhibitors, respectively.

The impedance parameters were obtained from the EIS measurements and the inhibition efficiency of C-steel in 1 M HCl solution with and without different concentrations of EJTLE, which are listed in Table 2. Specifically, when the inhibitor concentration is $0.1 \text{ g}\cdot\text{L}^{-1}$, the charge transfer resistance increases from $19.02 \text{ }\Omega$ to $129.65 \text{ }\Omega$ in the blank solution at 298 K. Additionally, the double-layer capacitance is reduced from $198.3 \text{ F}\cdot\text{cm}^{-2}$ to $92.8 \text{ F}\cdot\text{cm}^{-2}$. This phenomenon indicates the formation of an adsorbed layer, which slows the rate of carbon corrosion. The results show that the plant inhibitors have enhanced corrosion resistance and can be used as efficient inhibitors for the pickling and descaling of C-steel.

Table 2. The impedance parameters for C-steel in 1 M HCl solution with and without various concentrations of EJTLE at different temperatures.

Temperature (K)	CEJTLE ($\text{g}\cdot\text{L}^{-1}$)	R_s ($\Omega\cdot\text{cm}^{-2}$)	R_{ct} ($\Omega\cdot\text{cm}^{-2}$)	$\text{CPE-T}/Y_0 \times 10^6$ ($\Omega^{-1}\cdot\text{cm}^{-2} \text{ s}^n$)	n	C_{dl} ($\mu\text{F}\cdot\text{cm}^{-2}$)	η (%)	f
298	0	0.98	19.02	290.95	0.93	198.3	-	37.56
	0.02	1.03	38.01	320.12	0.89	188.1	50.0	21.23
	0.04	1.23	75.25	217.26	0.89	128.1	74.7	21.23
	0.06	0.96	92.81	224.94	0.87	132.8	79.5	11.91
	0.08	1.07	219.20	143.46	0.91	102.4	91.3	8.071
	0.1	1.49	208.50	129.65	0.91	92.8	90.9	6.643
	0.2	1.02	573.00	123.90	0.78	66.6	96.7	3.742
	0.5	0.69	463.60	122.92	0.86	80.7	95.9	3.742
	0	1.09	10.48	440.74	0.90	238.8	-	81.38
308	0.02	1.01	13.94	347.00	0.91	196.4	24.8	81.38
	0.04	0.30	36.62	208.90	0.93	145.2	71.4	25.7
	0.06	0.77	42.60	491.82	0.82	229.7	75.4	14.36
	0.08	0.66	53.85	520.29	0.81	233.3	80.5	14.36
	0.1	0.62	59.74	434.35	0.84	236.7	82.5	8.071
	0.2	0.95	83.82	499.15	0.77	214.3	87.5	8.071
	0.5	0.59	82.66	351.67	0.81	174.3	87.3	8.071
	0	0.73	5.21	576.40	0.93	372.8	-	81.38
	0.02	0.89	6.91	675.58	0.88	316.1	24.5	81.38
318	0.04	0.63	10.13	564.93	0.89	310.3	48.6	46.5
	0.06	0.77	17.00	595.16	0.84	251.0	69.4	46.5
	0.08	0.95	26.48	416.01	0.86	206.1	80.3	25.7
	0.1	0.66	43.92	383.54	0.85	200.5	88.1	14.36
	0.2	0.74	45.80	463.03	0.81	206.0	88.6	14.36
	0.5	0.44	46.90	547.17	0.77	211.0	88.9	14.36

Base on the θ values obtained from the EIS measurements, the mechanism of the EJTLE inhibitors on the C-steel in 1 M solution can be described by the Langmuir adsorption model [33]:

$$\frac{C_{inh}}{\theta} = \frac{1}{K_{ads}} + C_{inh} \quad (5)$$

where K_{ads} is the adsorption equilibrium constant, C_{inh} is the inhibitor concentration, and θ ($\eta/100$) is the coverage of the adsorbed inhibitors on the C-steel. The linearized mathematical expression has been obtained by the experimental data as follows:

$$y_1 = 1.01173x_1 + 0.01443 \quad R^2 = 0.99878 \quad (6)$$

$$y_2 = 1.08728x_2 + 0.04690 \quad R^2 = 0.98894 \quad (7)$$

$$y_3 = 1.04634x_3 + 0.04866 \quad R^2 = 0.98716 \quad (8)$$

Here, y and x represent the values of C_{inh}/θ and C_{inh} , respectively. The adsorption equilibrium constants obtained from the above-mentioned fitting relationship are $70.11 \text{ L}\cdot\text{g}^{-1}$, $23.18 \text{ L}\cdot\text{g}^{-1}$, and $21.50 \text{ L}\cdot\text{g}^{-1}$, respectively. Moreover, the standard adsorption free energy (ΔG_{ads}^0) is calculated by the following formula [34–36]:

$$K_{\text{ads}} = \frac{1}{55.5} \exp\left(\frac{-\Delta G_{\text{ads}}^0}{RT}\right) \quad (9)$$

where K_{ads} is also the adsorption equilibrium constant, R is the gas constant, and T is the absolute temperature, respectively. The values of the standard adsorption free energy obtained from the calculation was $-20.48 \text{ kJ}\cdot\text{mol}^{-1}$, $-18.33 \text{ kJ}\cdot\text{mol}^{-1}$, and $-18.73 \text{ kJ}\cdot\text{mol}^{-1}$, respectively. Namely, the results indicated that the type of adsorption of the plant inhibitors on the C-steel surface is physical adsorption.

The FT-IR results explain the physical adsorption of the inhibitors on the surface of C-steel. Figure 8 shows that the *Eriobotrya japonica* Thunb. leaf extracts contain C, N, and O atoms in functional groups O–H, N–H, C=C, C–H, C–N, and C–O. These functional groups are effective adsorption centers that adsorbed on the C-steel surface and increased the charge transfer resistance to further retard the corrosion of C-steel.

According to the relevant literature, *Eriobotrya japonica* Thunb. leaves contain ursolic acid, oleanolic acid, and flavonoids. The structures of these molecules contain heteroatoms and benzene rings. The incompletely filled d electron orbitals of iron can interact with the lone electrons of polar groups in the inhibitors. The corrosion inhibitors form a compact protective film on the surface of C-steel, thus slowing down the corrosion rate of C-steel in HCl solution.

The use of extracts of highly prevalent plants may be an environmentally friendly and economical way to produce corrosion inhibitors. This method not only avoids the use of non-biodegradable, environmentally harmful inhibitors but it can also provide an efficient use for plants. As a result, researchers have studied plant extract inhibitors, and the results show that some natural plant extracts have significant corrosion inhibition efficiency. However, few studies have investigated the chemical constituents of plant extracts. There are many kinds of chemical constituents in plant extracts, and their compositions are quite different. It is worth mentioning that the properties of some components in the inhibitors may change in the acid solution. It is difficult to accurately analyze the composition of plant extracts and inhibitors. Therefore, even though experiments have proved that some plant extracts have high corrosion inhibition efficiency, there will still be doubts about the rationality of plant extract inhibitors.

Therefore, researchers should pay more attention to the inhibition effect of the main components in the extracts and explore the influence of the inhibitor extraction and preservation methods on the inhibition efficiency. Consequently, a deeper theoretical analysis should be carried out for corrosion inhibitors. In this paper, we conclude that *Eriobotrya japonica* Thunb. leaf extracts have a good corrosion inhibition effect on C-steel. The results of this study will provide sound scientific references for future studies.

4. Materials and Methods

4.1. Inhibitors and Electrode Preparation

Fresh *Eriobotrya japonica* Thunb. leaves were rinsed with tap water, dried in an oven at 323 K for 24 h, and ground into powder. A sample of 37.45 g of powdered leaves was dispersed in 1.0 L water and heated at 363 K for 1 h. The mixture was filtered, and a clear brown solution was dried in an oven at 353 K to obtain 5.31 g of powder.

Q235 C-steel (0.14% C, 0.19% Si, 0.55% Mn, 0.028% P, 0.020% S, and Fe balance) specimens, with dimensions of $1.0 \text{ cm} \times 1.0 \text{ cm} \times 0.3 \text{ cm}$ and $0.5 \text{ cm} \times 0.5 \text{ cm} \times 0.3 \text{ cm}$ were prepared for electrochemical and surface characterization studies. All metal specimens were polished carefully with emery paper (grade 400-600-800-1000, MATADOR, Remscheid, Germany) and rinsed with distilled water and ethanol

before the experiment. The HCl solution was prepared by diluting a concentrated HCl solution (37%) with distilled water. The concentration ranges of EJTLE varied from 0.02 to 0.5 g·L⁻¹.

4.2. Electrochemical Measurements

All electrochemical experiments were performed with a CHI660B electrochemical workstation (CHI Co., Shanghai, China) in a conventional three-electrode cell system with Q235 C-steel (1.0 cm × 1.0 cm) embedded in epoxy resin holders as the working electrode (WE), a platinum gauze as the counter electrode (CE), and a silver-silver chloride (Ag/AgCl) electrode (saturation concentration KCl) with a Luggin-Haber capillary as the reference electrode (RE). In this test, all electrochemical experiments were conducted after the metal specimens were immersed in 1 M HCl solution at open circuit potential (OCP) for 1 h until a steady state was obtained. The potentiodynamic polarization experiments employed the following parameter: scanning from −300 to +300 mV (versus OCP) at a scanning rate of 0.5 mV·s⁻¹. The electrochemical impedance spectra were measured at OCP with 10 mV AC amplitude over a frequency range of 100 kHz to 10 mHz. EIS data analysis was performed via ZView 3.0 version software (Scribner Associates Inc., Southern Pines, NC, USA).

4.3. Morphology Analysis

The corrosion microscopy of the C-steel surface before and after immersion in 1 M HCl solution with and without 0.5 g·L⁻¹ EJTLE at different temperatures for 1 h was characterized by TESCAN MIRA 3 (TESCAN, Brno, Czech Republic) scanning electronic microscopy (SEM). The accelerating voltage for SEM was 15 kV. In addition, FT-IR analysis (KBr pellet method) was performed with a Nicolet iS50 FT-IR Spectrometer (Thermo Fisher Scientific, Waltham, MA, USA) to characterize the product structure of EJTLE.

5. Conclusions

In this paper, electrochemical and surface characterization experiments were conducted to investigate the anti-corrosion effects of *Eriobotrya japonica* Thunb. leaf extracts as corrosion inhibitors for carbon steel in a hydrochloric acid pickling solution. The results show that the inhibitors form a barrier layer on the carbon steel surface by physical adsorption, thus inhibiting the cathodic hydrogen evolution and anodic dissolution reactions. Moreover, *Eriobotrya japonica* Thunb. leaf extracts are effective mixed-type corrosion inhibitors.

Acknowledgments: This work is supported by the National Natural Science Foundation of China (No. 61271059), the Natural Science Foundation Project of Chongqing (No. 2010BB4246), the Student Research Training Program (No. CQU-SRTP-20163360), and the Graduate Students Research Project of Chongqing (No. CXB14220). We thank LetPub (www.letpub.com) for its linguistic assistance during the preparation of this manuscript.

Author Contributions: Xueming Li, Qihui Wang and Wenjing Yang conceived and designed the experiments; Ke Xu, Yanjun Yin and Hebin Bao performed the experiments; Lidan Niu analyzed the data; Shiqi Chen wrote the paper.

Conflicts of Interest: The authors declare no conflicts of interest.

References

1. Singh, A.K.; Quraishi, M.A. Investigation of the effect of disulfiram on corrosion of mild steel in hydrochloric acid solution. *Corros. Sci.* **2011**, *53*, 1288–1297. [[CrossRef](#)]
2. Mert, B.D.; Yüce, A.O.; Kardas, G.; Yazıcı, B. Inhibition effect of 2-amino-4-methylpyridine on mild steel corrosion: Experimental and theoretical investigation. *Corros. Sci.* **2014**, *85*, 287–295. [[CrossRef](#)]
3. Solomon, M.M.; Umoren, S.A.; Udosoro, I.I.; Udoh, A.P. Inhibitive and adsorption behaviour of carboxymethyl cellulose on mild steel corrosion in sulphuric acid solution. *Corros. Sci.* **2010**, *52*, 1317–1325. [[CrossRef](#)]
4. Abiola, O.K.; Otaigbe, J.O.E.; Kio, O.J. *Gossipium hirsutum* L. extracts as green corrosion inhibitor for aluminum in NaOH solution. *Corros. Sci.* **2009**, *51*, 1879–1881. [[CrossRef](#)]

5. Torres, V.V.; Amado, R.S.; De Sá, C.F.; Fernandez, T.L.; Da Silva Riehl, C.A.; Torres, A.G.; D'Elia, E. Inhibitory action of aqueous coffee ground extracts on the corrosion of carbon steel in HCl solution. *Corros. Sci.* **2011**, *53*, 2385–2392. [[CrossRef](#)]
6. M'hiri, N.; Veys-Renaux, D.; Rocca, E.; Ioannou, I.; Boudhrioua, N.M.; Ghoul, M. Corrosion inhibition of carbon steel in acidic medium by orange peel extract and its main antioxidant compounds. *Corros. Sci.* **2016**, *102*, 55–62. [[CrossRef](#)]
7. El-Lateef, H.M.A.; Abo-Riya, M.A.; Tantawy, A.H. Empirical and quantum chemical studies on the corrosion inhibition performance of some novel synthesized cationic gemini surfactants on carbon steel pipelines in acid pickling processes. *Corros. Sci.* **2016**, *108*, 94–110. [[CrossRef](#)]
8. Li, L.; Zhang, X.; Lei, J.; He, J.; Zhang, S.; Pan, F. Adsorption and corrosion inhibition of Osmanthus fragran leaves extract on carbon steel. *Corros. Sci.* **2012**, *63*, 82–90.
9. Jokar, M.; Farahani, T.S.; Ramezanzadeh, B. Electrochemical and surface characterizations of morus alba pendula leaves extract (MAPLE) as a green corrosion inhibitor for steel in 1M HCl. *J. Taiwan Inst. Chem. Eng.* **2016**, *63*, 436–452. [[CrossRef](#)]
10. Satapathy, A.K.; Gunasekaran, G.; Sahoo, S.C.; Amit, K.; Rodrigues, P.V. Corrosion inhibition by Justicia gendarussa plant extract in hydrochloric acid solution. *Corros. Sci.* **2009**, *51*, 2848–2856. [[CrossRef](#)]
11. Chauhan, L.R.; Gunasekaran, G. Corrosion inhibition of mild steel by plant extract in dilute HCl medium. *Corros. Sci.* **2007**, *49*, 1143–1161. [[CrossRef](#)]
12. Soltani, N.; Tavakkoli, N.; Khayatkashani, M.; Jalali, M.R.; Mosavizade, A. Green approach to corrosion inhibition of 304 stainless steel in hydrochloric acid solution by the extract of Salvia officinalis leaves. *Corros. Sci.* **2012**, *62*, 122–135. [[CrossRef](#)]
13. Deng, S.; Li, X. Inhibition by Ginkgo leaves extract of the corrosion of steel in HCl and H₂SO₄ solutions. *Corros. Sci.* **2012**, *55*, 407–415. [[CrossRef](#)]
14. Ji, G.; Anjum, S.; Sundaram, S.; Prakash, R. Musa paradisiaca peel extract as green corrosion inhibitor for mild steel in HCl solution. *Corros. Sci.* **2015**, *90*, 107–117. [[CrossRef](#)]
15. Mourya, P.; Banerjee, S.; Singh, M.M. Corrosion inhibition of mild steel in acidic solution by Tagetes erecta (Marigold flower) extract as a green inhibitor. *Corros. Sci.* **2014**, *85*, 352–363. [[CrossRef](#)]
16. Bentrach, H.; Rahali, Y.; Chala, A. Gum Arabic as an eco-friendly inhibitor for API 5L X42 pipeline steel in HCl medium. *Corros. Sci.* **2014**, *82*, 426–431. [[CrossRef](#)]
17. Garai, S.; Garai, S.; Jaisankar, P.; Singh, J.K.; Elango, A. A comprehensive study on crude methanolic extract of Artemisia pallens (Asteraceae) and its active component as effective corrosion inhibitors of mild steel in acid solution. *Corros. Sci.* **2012**, *60*, 193–204. [[CrossRef](#)]
18. Abdel-Gaber, A.M.; Abd-El-Nabey, B.A.; Saadawy, M. The role of acid anion on the inhibition of the acidic corrosion of steel by lupine extract. *Corros. Sci.* **2009**, *51*, 1038–1042. [[CrossRef](#)]
19. Deng, S.; Li, X. Inhibition by Jasminum nudiflorum Lindl. leaves extract of the corrosion of aluminium in HCl solution. *Corros. Sci.* **2012**, *64*, 253–262. [[CrossRef](#)]
20. Li, X.; Deng, S. Inhibition effect of Dendrocalamus brandisii leaves extract on aluminum in HCl, H₃PO₄ solutions. *Corros. Sci.* **2012**, *65*, 299–308. [[CrossRef](#)]
21. Pereira, S.S.D.A.A.; Pêgas, M.M.; Fernández, T.L.; Magalhães, M.; Schöntag, T.G.; Lago, D.C.; de Senna, L.F.; D'Elia, E. Inhibitory action of aqueous garlic peel extract on the corrosion of carbon steel in HCl solution. *Corros. Sci.* **2012**, *65*, 360–366. [[CrossRef](#)]
22. Al-Sehaibani, H. Evaluation of extracts of Henna leaves as environmentally friendly corrosion inhibitors for metals. *Materialwiss. Werkstofftech.* **2000**, *31*, 1060–1063. [[CrossRef](#)]
23. Orubite, K.O.; Oforka, N.C. Inhibition of the corrosion of mild steel in hydrochloric acid solutions by the extracts of leaves of Nypa fruticans Wurmb. *Mater. Lett.* **2004**, *58*, 1768–1772. [[CrossRef](#)]
24. Abdel-Gaber, A.M.; Nabey, B.A.A.; Sidahmed, I.M.; El-Zayady, A.M.; Saadawy, M. Effect of temperature on inhibitive action of damsissa extract on the corrosion of steel in acidic media. *Corrosion* **2006**, *62*, 293–299. [[CrossRef](#)]
25. Bouyanzer, A.; Hammouti, B.; Majidi, L. Pennyroyal oil from Mentha pulegium as corrosion inhibitor for steel in 1M HCl. *Mater. Lett.* **2006**, *60*, 2840–2843. [[CrossRef](#)]
26. Ei-Etre, A.Y. Inhibition of acid corrosion of carbon steel using aqueous extract of olive leaves. *J. Colloid Interface Sci.* **2007**, *314*, 578–583. [[CrossRef](#)] [[PubMed](#)]

27. Chellouli, M.; Chebabe, D.; Dermaj, A.; Erramli, H.; Bettach, N.; Hajjaji, N.; Casaletto, M.P.; Cirrincione, C.; Privitera, A.; Srhiri, A. Corrosion inhibition of iron in acidic solution derived from *Nigella sativa* L. by a green formulation. *Electrochim. Acta* **2016**, *204*, 50–59. [[CrossRef](#)]
28. Matalka, K.Z.; Abdulridha, N.A.; Badr, M.M.; Mansoor, K.; Qinna, N.A.; Qadan, F. Eriobotrya japonica Water Extract Characterization: An Inducer of Interferon-Gamma Production Mainly by the JAK-STAT Pathway. *Molecules* **2016**, *21*, 722. [[CrossRef](#)] [[PubMed](#)]
29. Detommasi, N.; Desimone, F.; Pizza, C.; Mahmood, N.; Moore, P.S.; Conti, C.; Orsi, N.; Stein, M.L. Constituents of eriobotrya-japonica—a study of their antiviral properties. *J. Nat. Prod.* **1992**, *55*, 1067–1073. [[CrossRef](#)]
30. Cheng, L.; Liu, Y.; Chen, L.; Luo, J. Studies on the triterpenoidal saponins from flowers of *Eriobotrya japonica*. *J. West China Univ. Med. Sci.* **2001**, *32*, 283–285.
31. Yan, Y.; Li, W.; Cai, L.; Hou, B. Electrochemical and quantum chemical study of purines as corrosion inhibitors for mild steel in 1M HCl solution. *Electrochim. Acta* **2008**, *53*, 5953–5960. [[CrossRef](#)]
32. Li, W.H.; He, Q.; Zhang, S.T.; Pei, C.L.; Hou, B.R. Some new triazole derivatives as inhibitors for mild steel corrosion in acidic medium. *J. Appl. Electrochem.* **2007**, *38*, 289–295. [[CrossRef](#)]
33. Abdallah, Y.M. Electrochemical studies of phenyl sulphonyl ethanone derivatives compounds on corrosion of aluminum in 0.5 M H₂SO₄ solutions. *J. Mol. Liq.* **2016**, *219*, 709–719. [[CrossRef](#)]
34. Bahrami, M.J.; Hosseini, S.M.A.; Pilvar, P. Experimental and theoretical investigation of organic compounds as inhibitors for mild steel corrosion in sulfuric acid medium. *Corros. Sci.* **2010**, *52*, 2793–2803. [[CrossRef](#)]
35. Ghareba, S.; Omanovic, S. 12-Aminododecanoic acid as a corrosion inhibitor for carbon steel. *Electrochim. Acta* **2011**, *56*, 3890–3898. [[CrossRef](#)]
36. Qiang, Y.; Zhang, S.; Guo, L.; Zheng, X.; Xiang, B.; Chen, S. Experimental and theoretical studies of four allyl imidazolium-based ionic liquids as green inhibitors for copper corrosion in sulfuric acid. *Corros. Sci.* **2017**, *119*, 68–78. [[CrossRef](#)]



© 2017 by the authors. Licensee MDPI, Basel, Switzerland. This article is an open access article distributed under the terms and conditions of the Creative Commons Attribution (CC BY) license (<http://creativecommons.org/licenses/by/4.0/>).